J|A|C|S ARTICLES

Published on Web 03/31/2010

Half-Metallic Ferromagnetism and Large Negative Magnetoresistance in the New Lacunar Spinel $GaTi_3VS_8$

Eugen Dorolti,[‡,¶] Laurent Cario,[*,†,‡] Benoît Corraze,[†,‡] Etienne Janod,[†,‡] Cristian Vaju,[‡] Hyun-Joo Koo,[§] Erjun Kan,[⊥] and Myung-Hwan Whangbo[⊥]

Institut des Materiaux Jean Rouxel (IMN), Université de Nantes, CNRS, 2, rue de la Houssinière, BP 32229, 44322 Nantes Cedex 3, France, Department of Chemistry and Research Institute of Basic Science, Kyung Hee University, Seoul 130-701, Korea, and Department of Chemistry, North Carolina State University, Raleigh, North Carolina 27695-8204

Received September 24, 2009; E-mail: Laurent.Cario@cnrs-imn.fr

Abstract: The lacunar spinel compounds $GaTi_{4-x}V_xS_8$ ($0 < x < 4$), consisting of $Ti_{4-x}V_x$ tetrahedral clusters, were prepared and their structures were determined by powder X-ray diffraction. The electronic structures of $GaTi_{4-x}V_xS_8$ ($x = 0, 1, 2, 3$) were examined by density functional calculations, and the electrical resistivity and magnetic susceptibility of these compounds were measured. Our calculations predict that $GaTi_3VS_8$ is a ferromagnetic half-metal, and this prediction was confirmed by magnetotransport experiments performed on polycrystalline samples of $GaTi_3VS_8$. The latter reveal a large negative magnetoresistance (up to 22% at 2 K), which is consistent with the intergrain tunnelling magnetoresistance expected for powder samples of a ferromagnetic half-metal and indicates the presence of high spin polarization greater than 53% in $GaTi_3VS_8$.

1. Introduction

During the last decades, transition metal Mott insulators were among the most studied compounds because they exhibit a variety of exotic phenomena when they are brought close to the metal−insulator transition (MIT) either by doping or by an external pressure.[1] High-T_c superconductivity in cuprates or colossal magnetoresistance in manganites are examples of such phenomena that occur when Mott insulators are doped. Recently, a family of Mott insulators, AM_4X_8 (A = Ga, Ge; M = V, Nb, Ta, Mo; X = S, Se) containing transition-metal tetrahedral clusters (Figure 1), was discovered.[2,3] These AM_4X_8 compounds exhibit interesting properties close to their MIT. For example, $GaTa_4Se_8$ is a rare example of Mott insulator that undergoes a MIT and becomes a superconductor under pressure.[4,5] Furthermore, $GaTa_4Se_8$ exhibits an electric-pulse-induced MIT associated with an electronic phase separation.[6−8]

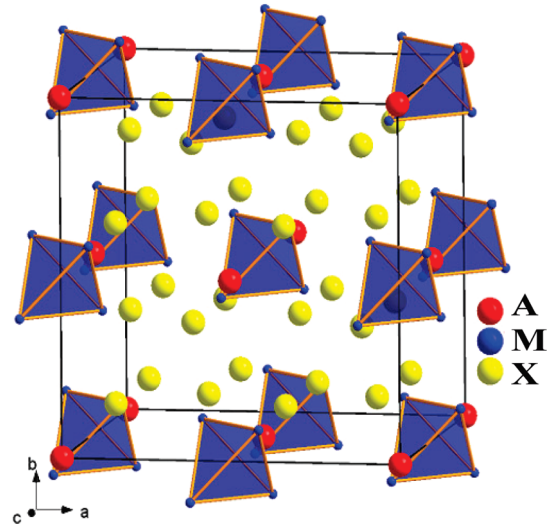

Figure 1. Perspective view of the crystal structure of AM_4X_8 (A = Ga, Ge; M = V, Nb, Ta, Mo; X = S, Se). The M_4 tetrahedral clusters are presented as blue tetrahedra.

The lacunar spinel compound $GaTi_4S_8$ with three valence electrons per Ti_4 tetrahedral cluster is a metal,[9] while GaV_4S_8 with seven electrons per V_4 tetrahedral cluster is a Mott

[†] These authors contributed equally to this work.
[‡] Université de Nantes.
[§] Kyung Hee University.
[⊥] North Carolina State University.
[¶] Current address: Physics Faculty "Babes-Bolyai" University, Department of Physics of Advanced Materials and Technology, Mihail Kogalniceanu, Nr. 1 RO-400084, Cluj-Napoca, Romania.

(1) Imada, M.; Fujimori, A.; Tokura, Y. *Rev. Mod. Phys.* **1998**, *70*, 1039.
(2) Johrendt, D. *Z. Anorg. Allg. Chem.* **1998**, *624*, 952–958.
(3) Ben Yaich, H.; Jegaden, J. C.; Potel, M.; Sergent, M.; Rastogi, A. K.; Tournier, R. *J. Less-Common Met.* **1984**, *102*, 9.
(4) Abd-Elmeguid, M. M.; Ni, B.; Khomskii, D. I.; Pocha, R.; Johrendt, D.; Wang, X.; Syassen, K. *Phys. Rev. Lett.* **2004**, *93*, 126403.
(5) Pocha, R.; Johrendt, D.; Ni, B. F.; Abd-Elmeguid, M. M. *J. Am. Chem. Soc.* **2005**, *127*, 8732–8740.
(6) Vaju, C.; Cario, L.; Corraze, B.; Janod, E.; Dubost, V.; Cren, T.; Roditchev, D.; Braithwaite, D.; Chauvet, O. *Adv. Mater.* **2008**, *20*, 2760–2765.
(7) Vaju, C.; Cario, L.; Corraze, B.; Janod, E.; Dubost, V.; Cren, T.; Roditchev, D.; Braithwaite, D.; Chauvet, O. *Microelectron. Eng.* **2008**, *85*, 2430.
(8) Dubost, V.; Cren, T.; Vaju, C.; Cario, L.; Corraze, B.; Janod, E.; Roditchev, D. *Adv. Funct. Mater.* **2009**, *19*, 2800–2804.
(9) Vaju, C.; Martial, J.; Janod, E.; Corraze, B.; Fernandez, V.; Cario, L. *Chem. Mater.* **2008**, *20*, 2382–2387.

10.1021/ja908128b

Table 1. Crystallographic Data and Results of Rietveld Refinements Performed on X-ray Powder Patterns Collected for $GaTi_{4-x}V_xS_8$ ($0 \leq x \leq 4$)

formula	$Ga_{0.85}Ti_4S_8$	$Ga_{0.89}Ti_3VS_8$	$GaTi_2V_2S_8$	$GaTiV_3S_8$	GaV_4S_8
space group	$F\bar{4}3m$	$F\bar{4}3m$	$F\bar{4}3m$	$F\bar{4}3m$	$F\bar{4}3m$
symmetry	cubic	cubic	cubic	cubic	cubic
no. of refined parameters	16	16	16	16	16
2θ range (deg)	10−120	10−120	10−120	10−120	10−120
a (Å)	9.9020(5)	9.8558(4)	9.7973(2)	9.7219(2)	9.6540(3)
V (Å^3)	970.88(9)	957.36(6)	940.42(4)	918.87(3)	899.74(5)
Z	4	4	4	4	4
R_{Bragg} (%)	4.64	4.54	2.92	4.10	3.11
R_P (%)	5.72	4.95	5.25	4.93	3.86
R_{wp} (%)	7.61	6.29	7.43	6.86	5.32
U_{iso} (Ga) (Å^2)	0.0075(1)	0.0096(1)	0.0077(9)	0.0067(1)	0.0070(9)
U_{iso} (V) (Å^2)	0.0087(5)	0.0105(4)	0.0103(5)	0.0084(5)	0.0081(4)
U_{iso} (Ti) (Å^2)	0.0087(5)	0.0105(4)	0.0103(5)	0.0084(5)	0.0081(4)
U_{iso} (S1) (Å^2)	0.0056(9)	0.0064(8)	0.0101(8)	0.0079(9)	0.0072(8)
U_{iso} (S2) (Å^2)	0.0078(1)	0.0124(1)	0.0081(9)	0.0059(1)	0.0111(1)
x (Ga)	0	0	0	0	0
x (Ti/V)	0.6144(1)	0.6115(9)	0.6095(1)	0.6072(1)	0.6063(8)
x (S1)	0.3725(3)	0.3710(3)	0.3719(5)	0.3717(8)	0.3695(4)
x (S2)	0.8690(4)	0.8685(4)	0.8659(6)	0.8639(8)	0.8651(5)
d_{M-M} (Å)	3.2019(4)	3.1010(3)	3.0312(4)	2.9410(6)	2.9016(2)
d_{M--M} (Å)	3.8018(4)	3.8610(3)	3.8915(4)	3.9304(6)	3.9218(2)
d_{M-x} (Å)	2.4018(7)	2.3812(6)	2.3418(8)	2.3080(2)	2.3115(6)
d_{M--x} (Å)	2.5316(8)	2.5415(6)	2.5310(8)	2.5280(2)	2.5206(7)

insulator.[10] Thus, one might wonder if a doping-induced MIT might occur in $GaTi_{4-x}V_xS_8$ ($x = 1-3$), if it were to possess $Ti_{4-x}V_x$ tetrahedral clusters. In our attempt to explore this possibility, we prepared the series of solid solutions $GaTi_{4-x}V_xS_8$ ($0 < x < 4$), determined their structures, and examined their electronic structures by density functional calculations. Our calculations predict that the phase $GaTi_3VS_8$ is a ferromagnetic half-metal; namely, it is metallic in one spin channel and insulating in another spin channel. We verify this prediction by carrying out electrical resistivity and magnetic susceptibility measurements for $GaTi_3VS_8$.

2. Experimental Details

Synthesis. All compounds were synthesized by solid-state reaction. The samples were prepared by heating stoichiometric mixtures of Ga, titanium, vanadium, and sulfur (purities >99.99%) in sealed glass tubes under small residual pressure (<10^{-2} bar) at the rate of 30 K/h to 1263 K, and keeping at 1263 K for 160 h. This synthesis yields dark gray powders, which show no reaction when exposed to air or humidity. These powders were reground, pressed into pellets and annealed at 1263 K for 24 h. This last step, which improves the purity of the samples, was performed once or twice depending on the sample purity. A similar result was obtained when using Ga_2S_3 instead of Ga as gallium precursor. In this case, a pure sample of Ga_2S_3 was first obtained by heating Ga_2O_3 at 1073 K for 8 h under H_2S flow.

Chemical Analysis. of all compounds was performed on powder samples using an electron microscope JEOL 5800LV equipped with an energy dispersive X-ray spectroscopy (EDXS) apparatus.

X-ray Diffraction. analysis of $GaTi_{4-x}V_xS_8$ powder samples were performed on a Bruker D8 Advance Diffractometer using Cu $K_{\alpha 1}$ radiation ($\lambda = 1.540598$ Å). Data were collected at room temperature in the 2θ range of 10−120° with acquisition time of 12 h. The cell parameters and the crystal structures were refined by the Rietveld method using the programs FullProf[11] and WinPlotr.[12] The background was fitted by a linear interpolation between selected points. All refinements used the March−Dollase model for preferred orientation and the pseudo-Voigt function for peak-shape model. The structure was refined by starting with the atomic coordinates found for $Ga_{1-\delta}Ti_4S_8$. When necessary we used a multiple-phase procedure to take into account a small amount of TiO_2 impurity (proportion <2 weight%). Since a Ga nonstoichiometry was found in the pure titanium compound, we have always tried to refine the site occupancy factor on the Ga site. This led in some cases to a further improvement of the refinement and a better agreement between analyzed and refined chemical formulas. We have also tried to refine a partial Ga-occupation of the second tetrahedral site, but this led to a site occupancy that did not depart from 0 within the standard deviation. All details about data collections, structure refinements, and refinement results are gathered in Table 1 (and Table S.1 in Supporting Information).

Electrical Resistivity. was measured on pressed pellets of $GaTi_{4-x}V_xS_8$ using a source-measure unit Keithley 236 with a four-point probe method. Four 50 μm gold wire electrodes were fixed on the pellets using a carbon paste and were annealed at 473 K for 2 h under vacuum. The measurements were performed between 300 and 1.5 K at bias smaller than 0.01 V. The resistance was also measured under magnetic field in the 0−5 T range using an Oxford cryostat equipped with a superconducting coil.

Magnetic Susceptibility. Measurements were performed on a Quantum Design MPMS-R5 SQUID magnetometer on powder samples of $GaTi_{4-x}V_xS_8$ (typical mass ∼100 mg) at 0.1 T in the temperature range 2−300 K. Raw data were corrected for the sample holder contribution and the core electron diamagnetism. For all concentrations, zero-field-cooled and field-cooled data are identical over the entire temperature range studied.

Theoretical Calculations. First-principles density functional theory (DFT) calculations were carried out by using the frozen-core projector augmented wave (PAW) method[13] encoded in the Vienna ab initio simulation package (VASP)[14] with the generalized gradient approximation (GGA)[15] for the exchange and correlation

(10) Muller, H.; Kockelmann, W.; Johrendt, D. *Chem. Mater.* **2006**, *18*, 2174–2180.

(11) Rodríguez-Carvajal, J. *FullProf 2000*; 2001; http://www.ill.eu/sites/fullprof.

(12) Roisnel, T.; Rodriguez-Carvajal, J. *Mater. Sci. Forum* **2001**, *378−381*, 118–123.

(13) Kresse, G.; Joubert, D. *Phys. Rev. B* **1999**, *59*, 1758.

(14) Kresse, G.; Furthmüller, J. *Vienna Ab-initio Simulation Package (VASP)*; Computational Physics, Faculty of Physics, Universität Wien: Wien, Austria, 2004; http://cms.mpi.univie.ac.at/vasp.

(15) Perdew, J. P.; Burke, S.; Ernzerhof, M. *Phys. Rev. Lett.* **1996**, *77*, 3865.

Table 2. Results of Chemical Analysis Performed for $GaTi_{4-x}V_xS_8$ ($0 \le x \le 4$) by Means of Energy Dispersive X-ray Spectroscopy

targeted composition	EDXS chemical analysis (at. %)				experimental composition[a]
	Ga	Ti	V	S	
$GaTi_3VS_8$	7.02	24.20	7.50	61.28	$Ga_{0.88}Ti_{3.05}V_{0.95}S_{7.73}$
$GaTi_2V_2S_8$	7.83	15.00	15.48	61.69	$Ga_{1.02}Ti_{1.97}V_{2.03}S_{8.10}$
$GaTiV_3S_8$	7.76	7.01	23.62	61.61	$Ga_{1.01}Ti_{0.92}V_{3.08}S_{8.05}$

[a] Sum of Ti and V fixed to 4.

correction. Our spin-polarized DFT calculations employed the plane-wave cutoff energy of 450 eV, the sampling of the irreducible Brillouin zone with 512 k-points, and the total energy convergence threshold of 10^{-6} eV. For the electronic structure of $GaTi_3VS_8$, we performed supercell calculations for several ordered structures as well as virtual crystal approximation (VCA) calculations using the SIESTA program.[16−19] In the latter calculations, only valence electrons are included, and the cores are replaced by a nonlocal norm-conserving Troullier−Martins pseudopotential[20] that was factorized in the Kleinman−Bylander form.[21]

3. Crystal structure

Our syntheses led to black powder samples whose chemical analyses were in good agreement with the targeted compositions (see Table 2). X-ray diffraction patterns (see Figure 2) revealed a complete solid solution between $GaTi_4S_8$ and GaV_4S_8. The shift of the diffraction peaks at high 2θ (see Figure 2) as well as our powder profile refinements show that the unit-cell parameter of the cubic spinel structure (SG F-43M) decreases continuously with increasing the V content from 9.9020(5) Å in $GaTi_4S_8$ to 9.6540(3) Å in GaV_4S_8 (see Table 1 and S1, Supporting Information). The structure of all compounds was refined by using the Rietveld method as described in the experimental section (see Tables 1 and S1 (Supporting Information) for details). Figure 3 presents a comparison of the observed and calculated $Ga_{1-\delta}Ti_{4-x}V_xS_8$ ($x = 1, 2, 3$) powder patterns. All substituted compounds $Ga_{1-\delta}Ti_{4-x}V_xS_8$ ($x = 1, 2, 3$) adopt the same deficient spinel structure as do the unsubstituted members $GaTi_4S_8$[9] and GaV_4S_8.[22] Difference Fourier maps do not reveal any electron density peaks that would indicate that V and Ti atoms are located in slightly shifted positions. Moreover, the atomic displacement parameters of the transition metal atoms are comparable to those of other atoms. This indicates that most tetrahedral clusters of $Ga_{1-\delta}Ti_{4-x}V_xS_8$ have the composition close to $Ti_{4-x}V_x$, and that there is no strong mixture of clusters with very different compositions (e.g., Ti_4 and V_4 clusters with the composition ratio $4-x:x$). Rietveld refinements indicate that the vanadium-poor samples ($0 < x < 1.5$) exhibit a slight Ga nonstoichiometry (see Tables 1 and S1 in the Supporting Information), which is consistent with our chemical analyses (see Table 2).

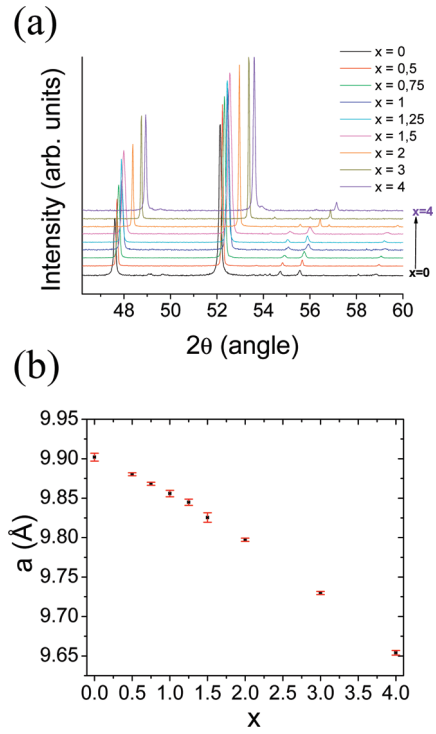

Figure 2. (a) X-ray powder patterns recorded for the series of compounds $GaTi_{4-x}V_xS_8$ ($x = 0-4$). (b) Evolution of the cell parameter a of $GaTi_{4-x}V_xS_8$ as a function of the vanadium content x. In this figure the error bars are multiplied by 10 compared to the refined value reported in Table 1 and S1 in the Supporting Information.

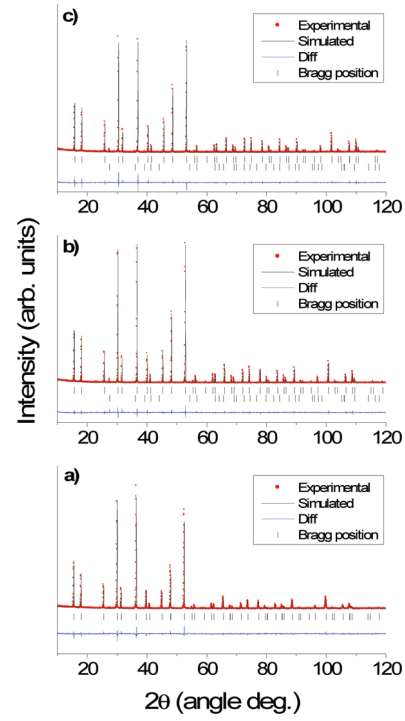

Figure 3. X-ray diffraction patterns observed for (a) $GaTi_3VS_8$, (b) $GaTi_2V_2S_8$ and (c) $GaTiV_3S_8$. The black lines represent the intensities calculated by the Rietveld method. The blue curve at the bottom represent the difference between the experimental and calculated intensities. The small marks indicate the Bragg peak positions of the target compounds (top) and of the impurity TiO_2 (bottom).

In $GaTi_{4-x}V_xS_8$ the Ga atoms are surrounded by four sulfur atoms in a tetrahedral environment, while the transition metal atoms M (= Ti or V) are located in a sulfur octahedral en-

(16) Artacho, E.; Gale, J. D.; García, A.; Junquera, J.; Martin, R. M.; Ordejón, P.; Sánchez-Portal, D.; Soler, J. M. *Siesta (Spanish Initiative for Electronic Simulations with Thousands of Atoms)*, v. 1.3; Siesta: Madrid, Spain, 2001.
(17) Soler, J. M.; Artacho, E.; Gale, J. D.; García, A.; Junquera, J.; Ordejón, P.; Sánchez-Portal, D. *J. Phys.: Condens. Matter* **2002**, *14*, 2745–2779.
(18) Artacho, E.; Sánchez-Portal, D.; Ordejón, P.; García, A.; Soler, J. M. *Phys. Status Solidi A* **1999**, *215*, 809–817.
(19) Sánchez-Portal, D.; Ordejón, P.; Artacho, E.; Soler, J. M. *Int. J. Quantum Chem.* **1997**, *65*, 453–461.
(20) Troullier, N.; Martins, J. L. *Phys. Rev. B* **1991**, *43*, 1993.
(21) Kleinman, L.; Bylander, D. M. *Phys. Rev. Lett.* **1982**, *48*, 1425.
(22) Pocha, R.; Johrendt, D.; Pottgen, R. *Chem. Mater.* **2000**, *12*, 2882–2887.

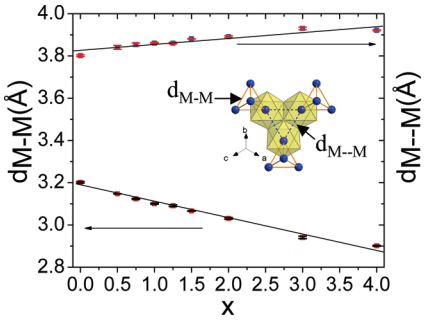

Figure 4. Intra- and intercluster metal−metal distances (M−M and M−−M, respectively) of $GaTi_{4-x}V_xS_8$ (M = Ti, V) as a function of x. The M−M and M−−M distances are defined in the inset. In this figure the error bars are multiplied by 10 compared to the refined value reported in Table 1 and S1 in the Supporting Information.

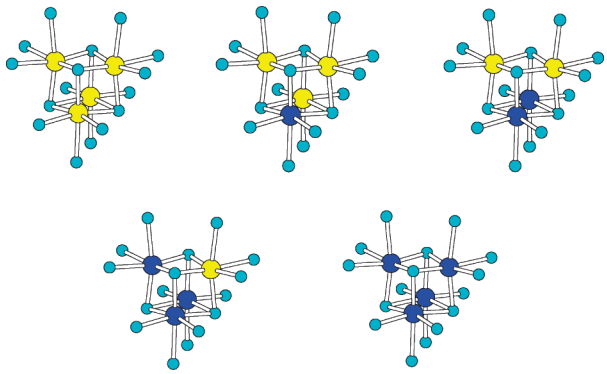

Figure 5. Schematic representations of the $Ti_{4-x}V_xS_{16}$ clusters in $GaTi_{4-x}V_xS_8$ (x = 0, 1, 2, 3, 4), where the blue, yellow, and cyan circles represent V, Ti, and S atoms, respectively.

vironment (see Figures 4 and 5). However, the transition metal atoms are strongly shifted from the center of these octahedral sites along the three-fold axis to form mixed-transition-metal tetrahedral clusters M_4 (see Figure 4), which leads to two kinds of metal−metal distances: the short intracluster M−M distance and the long intercluster distances M−−M. Figure 4 shows how these distances evolve through the series of compounds. With increasing the V content, the short intracluster M−M distance decreases continuously while the long intercluster distances M−−M increases continuously. This result shows that the transition-metal tetrahedral cluster shrinks in size on going from $GaTi_4S_8$ to GaV_4S_8.

4. Electronic Structure

In $GaTi_{4-x}V_xS_8$ (x = 0, 1, 2, 3, 4) the $Ti_{4-x}V_xS_{16}$ clusters (Figure 5) share the edges of their MS_6 (M = Ti, V) octahedra. Thus, the d-block bands of $GaTi_{4-x}V_xS_8$ are derived from the d-block levels of the $Ti_{4-x}V_xS_{16}$ clusters. The six low-lying d-block levels of the $Ti_{4-x}V_xS_{16}$ cluster in $GaTi_{4-x}V_xS_8$ (x = 0, 1, 2, 3, 4), obtained from extended Hückel tight binding calculations, are presented in Figure 6 (for the details of the atomic parameters employed, see Table S2 of the Supporting Information). The number of electrons, n, accommodated in these levels is n = 7 in GaV_4S_8, n = 6 in $GaTiV_3S_8$, n = 5 in $GaTi_2V_2S_8$, n = 4 $GaTi_3VS_8$, and n = 3 in $GaTi_4S_8$. Thus, with n = 7 and one electron to fill the triply degenerate level, GaV_4S_8 is a salient example of Mott insulator[10] with orbital degeneracy.

Electronic band structures of disordered compounds are difficult to simulate because one needs to consider a large number of possible structures. In principle, a given $GaTi_{4-x}V_xS_8$

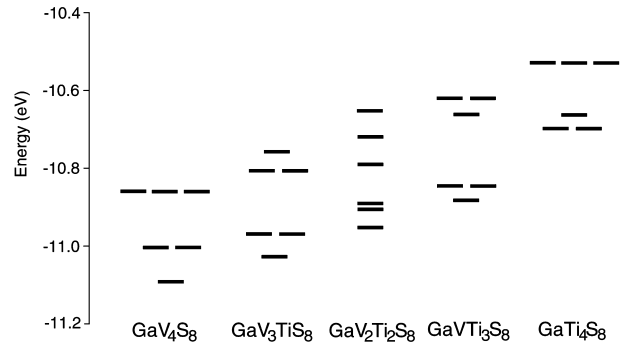

Figure 6. Six low-lying d-block levels of the $Ti_{4-x}V_xS_{16}$ cluster present in $GaTi_{4-x}V_xS_8$ (x = 0, 1, 2, 3, 4) obtained from extended Hückel tight binding calculations. The numbers of electrons n in these levels are: n = 7 in GaV_4S_8, n = 6 in $GaTiV_3S_8$, n = 5 in $GaTi_2V_2S_8$, n = 4 in $GaTi_3VS_8$, and n = 3 in $GaTi_4S_8$.

compound has a large number of possible structures with different arrangements of tetrahedral clusters with a same composition and/or different compositions. However, as discussed in the previous section, our X-ray analysis does not support a random distribution of clusters with different compositions, but suggests random orientations of clusters with a same composition. For this reason, we have excluded the case of a mixture of clusters with different compositions in all our band structure calculations. We have simulated the structures of $GaTi_4S_8$, $GaTi_3VS_8$, $GaTi_2V_2S_8$, and $GaTiV_3S_8$ by considering only arrangements of tetrahedral Ti_4, Ti_3V, Ti_2V_2, and TiV_3 clusters, respectively.

Spin-polarized GGA calculations carried out for $GaTi_4S_8$ and $GaTi_2V_2S_8$ show that they are regular metals in which both up-spin and down-spin d-block bands are partially filled. As can be seen from their density of state (DOS) plots (Figures S1.a and S1.b of the Supporting Information), the extent of spin polarization is not strong for $GaTi_4S_8$ and $GaTi_2V_2S_8$. The DOS plot (Figure S1.c in the Supporting Information) and the band dispersion relation (Figure S2 in the Supporting Information) of $GaTiV_3S_8$ show that it is a metal with a very small DOS at the Fermi level, which is understandable because each TiV_3S_{16} has six electrons to completely fill the bottom three d-block levels (Figure 6).

In contrast, our calculations predict $GaTi_3VS_8$ to be a ferromagnetic half-metal, i.e., it has partially filled bands in one spin channel (the up-spin bands by convention) but has a bandgap in the other spin channel (the down-spin bands by convention). This result was obtained by spin-polarized GGA performed on the most stable $GaTi_3VS_8$ structure (i.e., the arrangement A in Figure S3 in the Supporting Information), in which the tetrahedral Ti_3V clusters arranged to form "Ti_3V" intercluster tetrahedra. Our results for other arrangements of the tetrahedral Ti_3V clusters are summarized in Figures S3−S5 of the Supporting Information. That $GaTi_3VS_8$ is a ferromagnetic half-metal is also predicted by our VCA calculations, in which the random distribution of the Ti_3V cluster is simulated by replacing the Ti_3V with the hypothetical cluster T_4 such that the potential of the pseudoatom T is given by the weighted average of the potentials of one V and three Ti atoms (see Figure S6 of the Supporting Information). The total DOS plots, the partial DOS plots of the V 3d and Ti 3d states, and the band dispersion relations obtained from our spin-polarized GGA calculation on $GaTi_3VS_8$ are summarized in Figure 7. The up-spin bands have a bandgap at the Fermi level, while the down-spin bands are partially filled. The

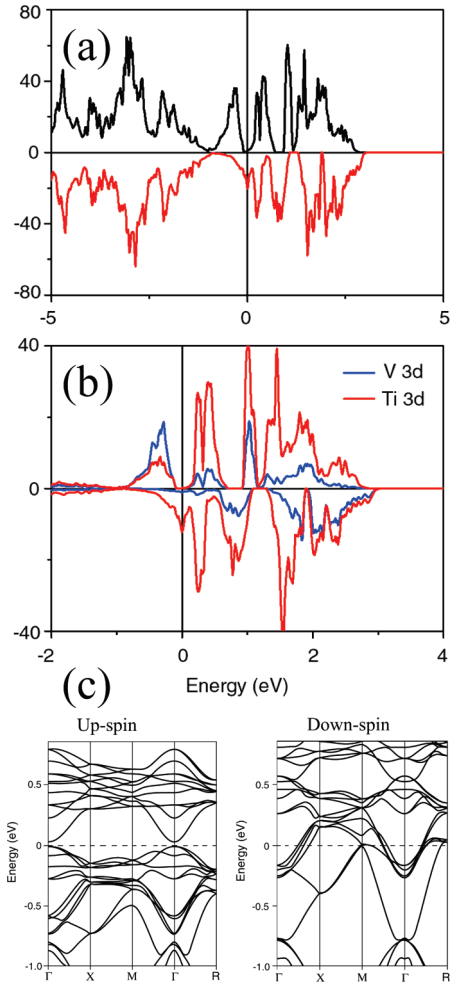

Figure 7. (a) Total DOS and (b) partial DOS plots obtained for the most stable arrangement of $GaTi_3VS_8$ (see arrangement A in Supporting Information) from spin-polarized GGA calculations. The up-spin and down-spin DOS plots are indicated by plus and minus values, respectively. (c) Dispersion relations of the d-block bands, around the Fermi level, calculated for $GaTi_3VS_8$ (arrangement A). In this figure, Γ = (0, 0, 0), X = (0.5, 0, 0), M = (0.5, 0.5, 0), R = (0.5, 0.5, 0.5), and the dashed lines indicate Fermi level.

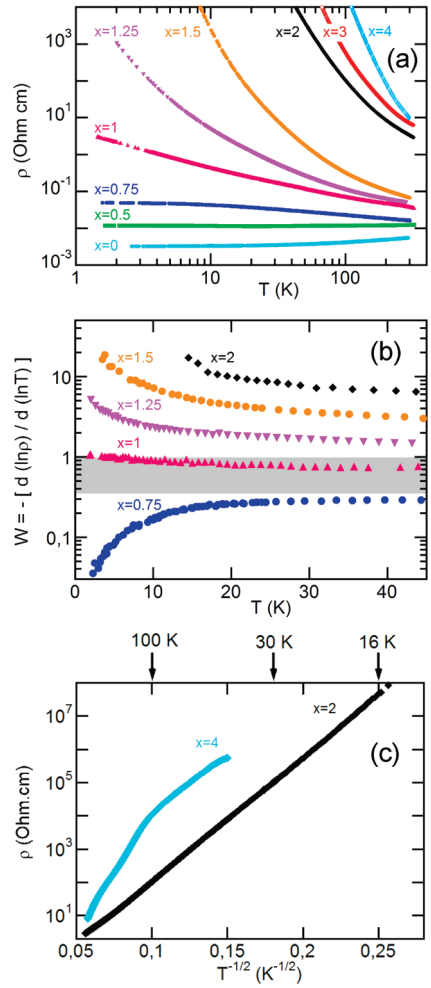

Figure 8. Electrical properties of $GaTi_{4-x}V_xS_8$ ($0 \le x \le 4$): (a) Temperature dependence of the resistivity measured for $GaTi_{4-x}V_xS_8$ ($0 \le x \le 4$). (b) Variation of the reduced activation energy W as a function of T, indicating that this metal−insulator transition is due to Anderson localization. The metal−insulator transition occurs at $x \approx 1$. (c) Variable-range hopping behavior of the resistivity, ln $\rho(T) \propto T^{-1/2}$, which is observed for $x = 2$ below 100 K, but not observed for $x = 4$.

magnetic moment of the structures obtained from this calculation is 2.01 μ_B per formula unit (FU). Thus, given the d-states of an isolated Ti_3V cluster (Figure 6) with four d-electrons to fill, our calculations predict an intermediate spin configuration. To summarize, our calculations predict a ferromagnetic half-metallic character for $GaTi_3VS_8$ with an intermediate spin configuration on the cluster.

5. Electrical Resistivity

All computed compounds $GaTi_{4-x}V_xS_8$ (x = 0, 1, 2, 3) are predicted to be metallic, and a MIT should occur in the vanadium-rich region ($3 < x < 4$). To probe this MIT we have measured the electrical resistivities for several members of the $GaTi_{4-x}V_xS_8$ ($0 \le x \le 4$) series in the temperature range of 1.5−300 K. The results are summarized in Figure 8. As already reported, GaV_4S_8 is insulating,[22] while $GaTi_4S_8$ is metallic.[9] Figure 8 shows that the solid solution $GaTi_{4-x}V_xS_8$ ($0 \le x \le 4$) undergoes a smooth transition from an insulating to a metallic ground state with x decreasing from 4 to 0; the room temperature resistivity drops from ∼10 ohm/cm for the vanadium-rich compounds ($(2 \le x \le 4)$ to 10^{-1}−10^{-3} ohm/cm in titanium-rich compounds ($0 \le x \le 1.5$)). The temperature dependence of the resistivity is characteristic of a metal (i.e., dρ/dt >0) for the titanium-rich compounds (x = 0 and 0.5), but an insulating behavior (i.e., dρ/dt <0) is observed for the vanadium-rich compounds ($2 \le x \le 4$). As a consequence, the MIT arises in the $0.75 < x < 1.5$ composition range. This observation differs substantially from the prediction of our band structure calculations that an MIT occurs in the vanadium-rich region ($3 < x < 4$). However, it should be noted that band structure calculations for $GaTi_{4-x}V_xS_8$ ($0 < x < 4$) were carried out for their ordered structures, and hence the effect of random potentials associated with the disordered arrangements of the V and Ti atoms within and between the $Ti_{4-x}V_x$ tetrahedra is not taken into consideration (e.g., see Figures 8 and S.1 in the Supporting Information). The latter might lead to an Anderson localization,[23] leading to an MIT. For a system with random potential, the resistivity in the critical regime between the metallic and insulator states is known to follow a power-law dependence on temperature, which is described by the Larkin−Khmelnitskii model[24] as

(23) Mott, N. F. *Metal-Insulator Transition*; Taylor &. Francis: London, 1974.
(24) Larkin, A. I.; Khmelnitskii, D. E. *Zh. Eksp. Teor. Fiz.* **1982**, *83*, 1140.

$$\rho(T) \approx \frac{e^2 p_F}{\hbar^2}\left(\frac{k_B T}{E_F}\right) \approx T^{-\beta}$$

with the critical exponent in the range of $0.33 < \beta < 1$. Therefore, as shown in ref 25, a convenient way of confirming the occurrence of an Anderson MIT is to plot the temperature dependence of the reduced activation energy, W, defined as

$$W = -T\left(\frac{\mathrm{d}\ln\rho(T)}{\mathrm{d}T}\right) = -\frac{\mathrm{d}\ln\rho}{\mathrm{d}\ln T}$$

This quantity is known to change from a negative slope in the insulating regime to a positive slope in the metallic regime, and is constant in the critical regime with $0.33 < \beta < 1$. The W vs T plots calculated for $GaTi_{4-x}V_xS_8$ ($0 < x < 4$) are presented in Figure 8b, which provides clear evidence that an Anderson MIT occurs in this series with a critical behavior obtained in the composition range $0.75 < x < 1$. Namely, the MIT observed in the $GaTi_{4-x}V_xS_8$ ($0 \le x \le 4$) series is driven by disorder effects. This means that $GaTi_{4-x}V_xS_8$ with $x \le 1$ is metallic, whereas that with $x > 1$ exhibit a density of states at the Fermi level but is insulating because these states are localized by the disorder. Figure 8c shows, for $x = 2$ as a representative example, that ln $\rho(T)$ varies as $T^{-1/2}$ below 100 K. Such dependence is expected for the variable range-hopping conduction mechanism in which electron localization is driven by both disorder and electron correlation effects.[26] The presence of electronic correlation in the solid solution $GaTi_{4-x}V_xS_8$ is not surprising since the end members $GaTi_4S_8$ and GaV_4S_8 are a strongly correlated metal and a Mott insulator, respectively. Overall, the picture of a MIT driven by disorder in $GaTi_{4-x}V_xS_8$ for $0.75 < x < 1$ is consistent with our band structure calculations.

6. Magnetic Susceptibility

To confirm the prediction of our calculations that $GaTi_3VS_8$ is a ferromagnetic half-metal, we investigated the magnetic properties of several members of the $GaTi_{4-x}V_xS_8$ ($0 \le x \le 4$) series. Figure 9 summarizes the magnetic properties of $GaTi_{4-x}V_xS_8$ as a function of x. The temperature dependence of the molar magnetic susceptibility $\chi(T,x)$ of $GaTi_{4-x}V_xS_8$ is shown in Figure 9a for various x values (for clarity, the molar magnetic susceptibility for some compositions are displayed in Supporting Information, Figure S7). As summarized in Table 3, the magnetic susceptibility $\chi(T)$ of all x can be described by a modified Curie−Weiss law, $\chi = \chi_0 + C/(T - \theta)$. The Weiss temperature θ is positive for $x = 0.75$ and 1, indicating the presence of dominant ferromagnetic interaction, while it becomes negative for $x \ge 1.25$ (see the inset of Figure 9a). Similarly, the $\chi T(T)$ plots of Figure 9b show a large increase in the value of χT around 10 K for $GaTi_3VS_8$ and $GaTi_{2.75}V_{1.25}S_8$, suggesting a ferromagnetic behavior. Consistent with this suggestion, the plots of the magnetization vs magnetic field measured for $GaTi_3VS_8$ and $GaTi_{2.75}V_{1.25}S_8$ exhibit a ferromagnetic-like hysteresis loop with a small coercive field, as presented in Figure 9c. The (effective) magnetic moment per cluster deduced from the $\chi(T)$ fit (see Table 3) or from the magnetization curve for $GaTi_3VS_8$ is lower than the magnetic moment calculated by DFT. However, the comparison of the calculated and experimental values (per cluster) is relevant only in a very simple case when the compound is a magnetic Mott insulator. The situation here is more complex since the band structure calculations and our resistivity measurements reveal a metallic ground state. In essence, our electrical and magnetic measurements support that $GaTi_{4-x}V_xS_8$ for $x \approx 1$ shows an itinerant ferromagnetism, in agreement with the prediction of our band structure calculations that $GaTi_3VS_8$ is a ferromagnetic half-metal.

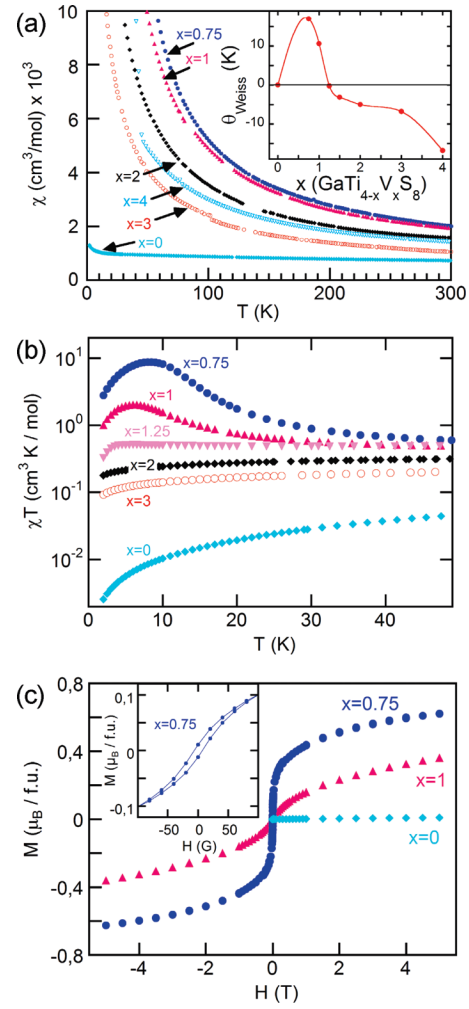

Figure 9. Magnetic properties of $GaTi_{4-x}V_xS_8$ ($0 \le x \le 4$): (a) Molar susceptibility χ of $GaTi_{4-x}V_xS_8$ ($0 \le x \le 4$) as a function of temperature. The inset shows the Weiss temperature, deduced from the fitting analysis of $\chi(T)$, as a function of x. (b) χT of $GaTi_{4-x}V_xS_8$ ($0 \le x \le 4$) as a function of temperature, which shows a Curie−Weiss behavior for $x \ne 0$ with dominant ferromagnetic interactions for $x = 0.75$ and 1.0, and with dominant antiferromagnetic interactions for $x = 2$ and 3. (c) Magnetization versus magnetic field measured at 2 K for $x = 0$, 0.75, and 1.0. The $x = 0$ sample shows no sign of ferromagnetism, whereas a ferromagnetic behavior appears for $x = 0.75$ and 1. The inset shows a zoomed-in view for $x = 0.75$.

Table 3. Parameters of the Modified Curie−Weiss law $\chi = \chi_0 + C/(T - \theta)$ Used to Fit the Magnetic Susceptibility of $GaTi_{4-x}V_xS_8$ ($0 \le x \le 4$); Effective Magnetic Moments μ_{eff} Deduced from C Are Also Listed

	fitting range (K)	χ_0 cm³ mol⁻¹	θ (K)	C_{exp} cm³ K mol⁻¹	μ_{eff} (μ_B)
$GaTi_4S_8$	–	1.25×10^{-3}	–	–	–
$GaTi_3VS_8$	20−300	6.84×10^{-4}	10.0	0.372	1.725
$GaTi_2V_2S_8$	20−300	4.81×10^{-4}	−4.1	0.318	1.595
$GaTiV_3S_8$	20−300	3.65×10^{-4}	−6.8	0.211	1.299
GaV_4S_8	50−300	4.88×10^{-4}	−16.1	0.290	1.523

(25) Zabrodskii, A. G.; Zeninova, N. *Zh. Eksp. Teor. Fiz.* **1984**, *86*, 727.
(26) Efros, A. L.; Shklovskii, B. I. *J. Phys. C* **1975**, *8*, L49.

7. Magnetoresistance

Ferromagnetic metals with large spin polarization are of great interest for spintronics applications.[27] As rewieved by Coey et al., ferromagnetic metals can arise from different situations.[28] The most simple one, is the occurrence of partially filled bands in one spin channel and a bandgap in the other spin channel such as in CrO_2.[28] However, a half-metallic behavior may also be observed in cases when the Fermi level cuts both spin direction bands but with one spin population localized and the other one delocalized. This situation is encountered, for example, in $(La_{0.7}Ca_{0.3})MnO_3$.[29] As suggested by our calculations and our resistivity measurements, both situations may be encountered in the compounds $GaTi_{4-x}V_xS_8$ with x close to 1. Indeed, our calculations predict a half-metal for $GaTi_3VS_8$ with partially filled bands in one spin channel and a bandgap in the other spin channel. Therefore, the compounds $GaTi_{4-x}V_xS_8$ with x close to 1 are good candidates to behave as half-metals with the current density carried predominantly by electrons of a single spin polarization. For this reason we have looked for evidence of a spin-polarized current in $GaTi_{4-x}V_xS_8$ ($x = 0.75$, 1). A direct consequence of the spin-polarized current in half-metals is the occurrence of a giant magnetoresistance when such compounds are incorporated into tunnelling junctions made up of two ferromagnetic metal layers separated by a nonmagnetic tunnelling barrier (e.g., MgO). Alternatively, a negative magnetoresistance (MR) can also be observed in polycrystalline samples of ferromagnetic metals.[30−32] A much simpler method to investigate the magnetotransport of half-metals and hence evidence of a spin-polarized current is therefore to perform powder MR measurements. Parts a and b of Figure 10 show the isothermal MR measured on pressed pellets of $GaTi_3VS_8$ and $GaTi_{3.25}V_{0.75}S_8$ at several temperatures ranging from 2 to 10 K. The negative MR (at 2 K under 5 T) is as large as 22% and 25% in $GaTi_3VS_8$ and $GaTi_{3.25}V_{0.75}S_8$, respectively. Interestingly, the MR's of $GaTi_3VS_8$ and $GaTi_{3.25}V_{0.75}S_8$ show a close correlation with the square of the magnetization at 2 K (see Figure 10c). This result is expected for an extrinsic MR related to a spin-dependent tunnelling between independent grains. In this case, the MR is related to the factor $\langle \cos^2 \theta \rangle \approx (M/M_s)^2$, where θ is the angle between the magnetization direction of the particles and the applied field, and M and M_s are the magnetization and the saturation magnetization, respectively. Since M_s is a constant, the MR is directly proportional to M^2. Therefore, the linear dependence of the MR on M^2 strongly suggests that the negative MR is due to the field enhancement of carrier tunnelling at the grain boundaries. As described in ref 22, the spin polarization P can be estimated from the measured MR from the relationship, $MR = P^2/(1 + P^2)$. Under 5 T, MR = 22 and 25% for $GaTi_3VS_8$ and $GaTi_{2.75}V_{1.25}S_8$, respectively, so that the polarization reaches 53% and 59% for $GaTi_3VS_8$ and $GaTi_{2.75}V_{1.25}S_8$, respectively. This is another clear sign, besides susceptibility, resistivity, and band structure calculations, that $GaTi_3VS_8$ and $GaTi_{2.75}V_{1.25}S_8$ are ferromagnetic half-metals.

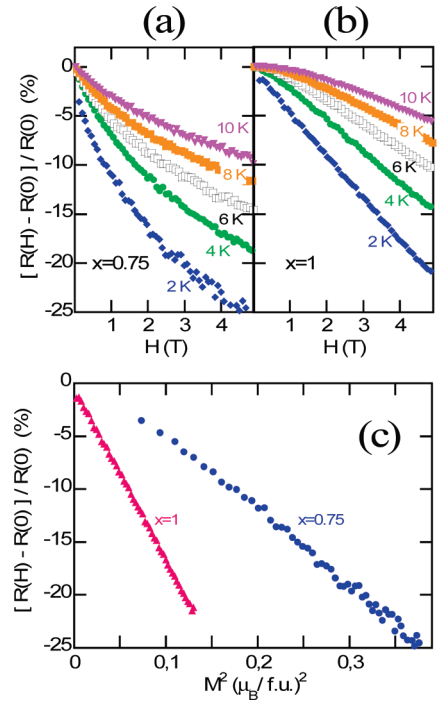

Figure 10. Magnetoresistance of $GaTi_{4-x}V_xS_8$. Magnetoresistance $[R(H) - R(0)]/R(0)$ of (a) $GaTi_3VS_8$ ($x = 1$) and (b) $GaTi_{3.25}V_{0.75}S_8$ ($x = 0.75$) measured at different temperatures ranging from 2 to 20 K. At 2 K under 5 T, the negative magnetoresistance reaches 22 and 25% for $GaTi_3VS_8$ and $GaTi_{3.25}V_{0.75}S_8$, respectively. (c) Linear dependence of the negative magnetoresistance on the square of the magnetization.

8. Concluding Remarks

We prepared and characterized the solid solution $GaTi_{4-x}V_xS_8$ ($0 < x < 4$) with lacunar spinel structure. The most striking features of this series of compounds are the occurrence of Anderson MIT for $0.75 < x < 1$ and a ferromagnetic half-metallic ground state for $x \approx 1$. For the latter composition, $GaTi_3VS_8$, a large negative MR (up to 22% at 2 K) is observed, hence leading to a high spin polarization greater than 53%. $GaTi_3VS_8$ is therefore a new compound exhibiting a ferromagnetic metallic ground state with large spin polarization.

Acknowledgment. E.D. thanks the region "Pays de la Loire" for providing a postdoctoral fellowship. The work at IMN was supported by a Young Researcher Grant ANR-05-JCJC-0123-01 from the French Agence Nationale de la Recherche (to L.C., B.C., and E.J.). The work at NCSU was supported by the Office of Basic Energy Sciences, Division of Materials Sciences, U.S. Department of Energy, under Grant DE-FG02-86ER45259 and by the resources of the NERSC center and the HPC center of NCSU.

Supporting Information Available: Rietveld refinements for compounds $GaTi_{4-x}V_xS_8$ with x close to 1 (Table S1). Calculation details, density of states, and band dispersions obtained for the $GaTi_{4-x}V_xS_8$ ($x = 0$, 1, 2, 3) compounds (Table S2; Figures S1−S6). Magnetic susceptibilities measured for compounds $GaTi_{4-x}V_xS_8$ with x close to 1 (Figure S7). X-ray crystallographic details supplied as CIF files. This material is available free of charge via the Internet at http://pubs.acs.org.

JA908128B

(27) Chappert, C.; Fert, A.; Ngyuen Van Dau, F. *Nat. Mater.* **2007**, *6*, 813–823.
(28) Coey, J. M. D.; Sanvito, S. *J. Phys. D: Appl. Phys.* **2004**, *37*, 988–993.
(29) Nadgorny, B.; Mazin1, I. I.; Osofsky, M.; Soulen, R. J., Jr.1; B., P.; Stroud, R. M.; Singh, D. J.; Harris, V. G.; Arsenov, A.; Mukovskii, Y. *Phys. Rev. B* **2001**, *63*, 184433.
(30) Coey, J. M. D. *J. Appl. Phys.* **1999**, *85*, 5576–5581.
(31) Coey, J. M. D.; Venkatesan, M. *J. Appl. Phys.* **2002**, *91*, 8345–8350.
(32) Xiao, J. Q.; Jiang, J. S.; Chien, C. L. *Phys. Rev. Lett.* **1992**, *68*, 3749.